ACCURATE PREDICTION OF HEAT PENETRATION OF A SURIMI PASTE WITH VARIOUS SALT AND MOISTURE CONTENTS USING NUMERICAL SIMULATION WITH TEMPERATURE DEPENDENT THERMAL PROPERTY FUNCTIONS

Hyeon Woo Park[(a)], Myeong-Gi Lee[(b)], Jae W. Park[(c)]
Won Byong Yoon[(d)]

[(a),(b),(d)] Department of Food Science and Biotechnology, College of Agricultural and Life Science, Kangwon National University, Chuncheon, Gangwon, 200-701, Republic of Korea
[(c)] 2001 Marine Drive, OSU Seafood Research and Education Center, Oregon State University, Astoria, OR 97103, USA

[(a)]hwpark0978@gmail.com, [(b)]mglee530@gmail.com, [(c)]surimiman1@yahoo.com
[(d)]wbyoon@kangwon.ac.kr

ABSTRACT
Alaska pollock surimi paste was prepared (0-3% salt and 76-84% moisture). The density, specific heat, and thermal conductivity have been measured and modelled in the temperature range 20-90°C. The density of AP surimi paste were represented by a multiple linear regression with respect to temperature, moisture and salt content with suitable R^2 value (0.92). The temperature and moisture and salt content dependence of a specific heat and thermal conductivity of surimi paste was well fitted with a multiple linear regression model with R^2 value of 0.97 and .087 respectively. The heat penetration curves measured during heating (25 to 90 °C) were compared with the transient temperature profile obtained from simulation models coupled with empirical thermal properties having suitable RMSE (0.43 to 1.22 °C). This study demonstrated that an accurate prediction of the heat transfer of the surimi paste needs tobe coupled with the nonlinear thermal property functions.

Keywords: Alaska Pollock, surimi, thermal property, numerical simulation

1. INTRODUCTION
Frozen surimi is a major ingredient to produce surimi seafood products (AbuDagga and Kolbe 1997, Park 2013). The frozen surimi block needs to be thawed, cut, and chopped with salt and water to prepare the surimi paste which may deform to various shapes of surimi seafood products (Fukushima et al. 2007, AbuDagga and Kolbe 2000). Surimi seafood products are conventionally made from heat set gels at high temperatures of approximately 90 °C (Tabilo-Munizaga and Barbosa-Cánovas, 2004). Accurate prediction of the heat transfer profile during processing is necessary to ensure the processing efficiency and the quality of products.
During the last three decades, computer simulation is becoming a powerful tool to interpret complex transport phenomena involved in many unit operations in food processing because of the fast development in the computational technologies as well as in the efficient numerical algorithms (Pitchai et al. 2014). Particularly, in recent years, many studies demonstrated that the numerical simulation (NS) were practically used in food processing operations, such as thermal processing, drying operation, and freezing (Scott and Richardson, 1997; Anandharamakrishnan 2003 and Norton and Sun 2006). Among many benefits of NS or CFD, the accurate estimation of the transient temperature profiles during thermal treatment would give a great benefit for food processing related to thermal processing. The estimation of transient temperature profile can be used to determine the cold point of food products thermally treated, and consequently the degree of sterilization is appropriately estimated. Including appropriate thermal properties in the heat transfer model is strongly required to obtain suitable transient temperature profiles from the NS (Scott and Richardson 1997, Anandharamakrishnan 2003). Although many advantages of using NS in food industry are found, there is no study related to the application of NS to understand the thermal processing involved in the surimi seafood which requires varied salt and moisture contents for commercial purposes. The NS for suimi paste needs a complicated heat transfer model because the thermal properties of surimi paste at different salt and moisture content could be significantly varied during heating process due to the interaction between compositions and the gelation of myofibrillar protein.
Because the thermal processing is the most important process to control the quality of surimi seafood, developing an accurate simulation models for surimi seafood processing may provide many advantages for the process engineers as well as the product developers. In addition, since the thermal process is one of the most costly aspects due to its high energy requirement, the accurately predicted thermal processing conditions will contribute to reduce the processing cost. Thus, it is worth to develop a suitable heat transfer models for surimi seafood with varied compositions such as salt and moisture. However, in order to develop an accurate and suitable model for the thermal process of surimi products, a thorough knowledge of the influence of the

individual component on thermal properties is essentially required. Especially, since the surimi paste inevitably contains salt and water, the thermal properties of surimi paste needs to be determined at various contents of salt and water in the paste. Therefore, the NS application should be accompanied with developing a semi- or empirical model to predict the temperature-dependent thermophysical properties, such as thermal conductivity k, specific heat C_p, and density ρ, of surimi paste at different salt and water levels in the wide range of temperature applied in the thermal processing of surimi seafood (AbuDagga and Kolbe 1997). Thermophysical properties of food are important parameters to determine appropriate operating conditions for various thermal processes including heating, cooking, freezing and cooling systems (Karunakar et al. 1998, Marcotte et al. 2008). In addition, the thermal properties are highly correlated to the degree of pasteurization or sterilization determining the shelf life of final products. Thus, it has been strongly emphasized to measure accurate thermal properties to ensure food safety (Unklesbay et al. 1999). We found no published reports on heat transfer properties of Alaska pollock surimi paste with considering the temperature dependence of thermal properties at various salt and moisture content, despite Alaska pollock still represents the largest fishery biomass used for surimi production (Guenneugues and Morrissey 2004). So far, the only published data on the thermal properties of surimi is limited to pacific whiting surimi of which production amount is only about 10% of Alaska Pollock surimi (AbuDagga and Kolbe 1997, Park 2013). Additionally, only one study on developing the heat transfer simulation model for AP surimi paste was recently reported by Lee and Yoon (2016), however the simulation model developed by Lee and Yoon (2016) was accompanied with constant thermal properties evaluated at a mean temperature during thermal processing. To develop an accurate heat transfer simulation model, thermal properties should be provided according to the temperature distribution of surimi during heating, and also those thermal properties must be evaluated at varied salt and moisture contents. To achieve an accurate heat transfer model to simulate the cooking process of surimi seafood made of AP surimi, the temperature dependent function of thermal properties at varied salt and moisture content must be developed and the functions has to be coupled with a governing equation of heat transfer. The objectives of this study were: (1) to investigate effects of salt and moisture content on thermal properties of AP surimi paste during heating, (2) to develop temperature dependent functions of AP surimi paste at varied salt and moisture content, and (3) to develop an accurate heat transfer simulation model of AP surimi paste coupled with variable thermal property functions to predict the transient temperature profiles in the surimi paste during heating.

2. MATERIALS AND METHODS

2.1. Materials and gel preparation

Alaska pollock (*Theragra chalcogramma*) surimi (A grade, 10 kg blocks), were provided from Trident Seafoods (Seattle, WA, USA) and kept in frozen at -18°C. Surimi pastes with 76, 80 and 84 % moisture content and 0, 1.5 and 3 % salt concentration were prepared as described by Yongsawatdigul et al. (1995). These compositions are mostly used in commercial surimi seafood products beside 0% of salt which was evaluated to characterize thermal properties of surimi itself. Frozen surimi blocks were thawed at room temperature for approximately 1 h and cut into cubes (5 cm). The initial temperature of surimi was about 2–3 °C. Surimi cubes were chopped with temperature control in a Stephan vacuum cutter (UM5, Stephan Machinery Co., Columbus, OH, USA) at low speed for 1 min. Salt content was adjusted to 0, 15, and 30) g kg^{-1} salt of total weight before chopping. Chopping at low speed was continued for 1 min. Ice was added to adjust the moisture concentration to (760, 800, and 840) g kg^{-1} and chopping continued an additional of 1 min on low speed (1800 rpm). Subsequently, samples were chopped at high speed (3600 rpm) for 3 min under vacuum to a final temperature of 4 °C. The paste was vacuum-packed in a plastic bag to eliminate air bubbles.

2.2. Thermal properties measurements

2.2.1. Density

Temperature dependence of the density of AP surimi paste was measured at four different temperatures (20, 30, 60, and 90 °C), according to AbuDagga and Kolbe (1997) and Lee and Yoon (2016). Surimi paste was extruded into a known size of stainless still tube (length of 17.5 cm; inner diameter of 1.9 cm). Surimi paste in the stainless still tube was placed in a controlled temperature water bath and allowed to expand freely as they gelled. At each heating temperature, the surimi gel expanded to the outside of the cylinder was trimmed off and the weight of the trimmed off part was accurately measured. Then the density was determined by weight of the surimi in the cylinder divided by the volume of the cylinder. Four replicates were used for each sample.

2.2.2. Thermal conductivity, specific heat and thermal diffusivity

Thermal conductivity and the specific heat of surimi pastes and gels were measured using a KD2 Pro Thermal Properties Analyzer (Decagon Devices Inc., Pullman, WA, USA), which is widely used to measure the thermal properties of food materials (Mahapatra et al. 2013). The dual needle SH-1 sensor (30 mm long, 1.28 mm diameter, and 6 mm spacing) measured the thermal conductivity and specific heat (heat capacity) concurrently at 25 °C and consequently from 30 to 90 °C every 10 °C interval. Ten replicates were performed for each sample. Thermal diffusivity of surimi pastes and gels were determined by following equation:

$$\alpha = \frac{k}{\rho C_p} \quad (1)$$

where α = thermal diffusivity (m^2/s); k = thermal conductivity (W m^{-1} $°C^{-1}$); ρ = density (kg/m^3); and C_p = specific heat (J kg^{-1} $°C^{-1}$).

2.3. Gelation with conventional water bath cooking

Heat treatment was conducted to the cube shape of surimi paste. The paste was molded into a cube shape molder (5 x 5 x 5 cm^3). After removing from the molder, the cube shapes of surimi paste were heated in a water bath (90 °C) for 60min. The temperature at the geometrical center was monitored using a T-type thermocouple probes (diameter 1.02 mm, Omega Engineering, Inc., Stanford, CT, USA) and recorded every 10 s using a Campbell 21X data-logger (Campbell Scientific Inc., Logan, UT, USA). The samples were kept in the water bath until the temperature at the center approached 90 °C. Triplicates were performed for each sample.

2.4. Numerical simulation

The differential equations of transient heat conduction are given by (Mohan and Talukdar 2010):

$$\rho(T, M, S)C_p(T, M, S)\frac{\partial T}{\partial t} = \nabla \cdot [k(T, M, S)\nabla T] \quad (2)$$

where T = product temperature (°C), M = product moisture content (%), S = product salt content (%) and t = time (s).

The initial condition for modeling is as follows:

$$t = 0, \mathrm{T} = T_0$$

and the boundary conditions are as follows:

$$x = 0, \frac{\partial T}{\partial x} = 0 \quad (3a)$$
$$y = 0, \frac{\partial T}{\partial y} = 0 \quad (3b)$$
$$z = 0, \frac{\partial T}{\partial z} = 0 \quad (3c)$$

and on the surface as follows:

$$-k(T, M, S)\left(\frac{\partial T}{\partial x}\right) = h(T_s - T_w) \quad (4a)$$
$$-k(T, M, S)\left(\frac{\partial T}{\partial y}\right) = h(T_s - T_w) \quad (4b)$$
$$-k(T, M, S)\left(\frac{\partial T}{\partial z}\right) = h(T_s - T_w) \quad (4c)$$

where T_s = the surface temperature (°C); T_w = the water bath temperature (°C); h = heat transfer coefficient (W m^{-1} $°C^{-1}$); x, y and z = distance in x, y and z-directions (m), respectively.

The heat transfer simulation was performed using the ANSYS workbench 16 program (ANSYS Inc., Canonsburg, PA, USA). The finite volume method using Ansys-Fluent module was employed to solve the three-dimensional heat transfer equation. The 4913 of meshes used in the geometry was determined at the constant RMSE values observed (Fig. 1b).

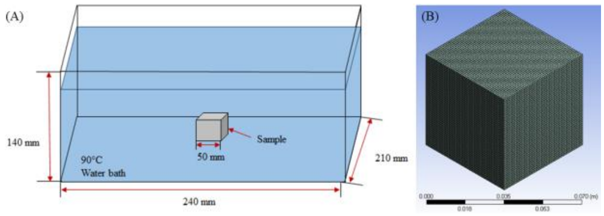

Figure 1: (a) The illustration of cooking of surimi paste in the water bath and (b) the 3-D geometrical model of the surimi block at 3 mm mesh size.

Transient 3D CFD simulation was performed with all side heating (wall temperature was set as T_{wall} = 90 °C). Initially surimi paste was at rest with uniform temperature of 18 ± 1.0 °C (based on the experiments). The hot water temperature (90 ± 0.5 °C) was remained constant. Calculations were performed on an Intel® Xeon® CPU E5-2690, 2.6 GHz PC (Intel Corporation, Santa Clara, CA, USA) with 256 Gbyte RAM running a Windows 10 64-bit edition (Microsoft, Redmond, WA, USA). The surimi paste was considered as non-Newtonian fluid, but it is considered as a semi-solid because of its high viscosity (Park 2013) and no applied shear stress. The properties of surimi paste (thermal conductivity, specific heat and density) was applied based on three different models.

- Model A - Constant value of each property at 30 °C

In model A, the thermal properties of surimi paste (thermal conductivity, specific heat and density) during simulation were constant values measured at 30 °C.

- Model B – the mean values of each thermal property during heating with consideration the phase transition were used for the simulation

Based on Lee and Yoon (2016), the mean values from the temperature penetration curves with consideration for the phase transition were used for Model B. A logistic model (Augusto et al., 2012).

$$f(t) = T_{max}/(1 + a \cdot e^{-b \cdot t}) \quad (5a)$$

where T_{max} = a constant value related to the equilibrium temperature; a = the constant; b = increase rate constant (s^{-1}); t = time (s). The mean temperature of each sample were calculated using eq. (5b) as follows"

$$\text{Mean temperature} = 1/(b - a)\int_a^b f(t)dt \quad (5b)$$

where $f(t)$ = temperature function of time. The temperature function was estimated using a logistic equation. The R^2 values of all logistic equations used in this study were higher than 0.99 (data were not shown). The sol-gel phase transition of surimi paste was considered based on the gelation temperature (40-50 °C) of surimi paste. The temperature was divided into three regions as follows: (1) lower than gelation temperature

(< 40 °C), (2) during gelation (40-50 °C), and (3) temperature higher than gelation temperature (> 50 °C). The thermal properties at the different mean values reflecting both phase transition and dimensions were used for the computer simulation.

- Model C – temperature-dependent functions of each property were coupled with the heat transfer model for the simulation.

The empirical models to predict the temperature-dependent properties (thermal conductivity, specific heat and density) of surimi were developed and used for the heat transfer simulations.

2.5. Calculation the heat transfer coefficient h

An average heat transfer coefficient, h, used in this study was estimated using dimensionless numbers. The film temperature was sued to evaluate all the fluid properties (Hong et al. 2014):

$$T_f = \frac{T_w + T_s}{2} \tag{6}$$

where T_f = film temperature (°C); T_w = the water bath temperature (°C); T_s = the surface temperature of sample (°C);. T_w was 90.0 °C, and T_s (18 °C) was the sample temperature before applying the heat treatment.

As the volume of the surimi samples (1.25×10^2 cm^3) is very small compared to that of the water bath (1.083×10^4 cm^3), the geometry governing the forced convection from the fluid is assumed to be an immersed horizontal plate (Geankoplis 2003). For an immersed horizontal plate geometry, Reynold number (N_{Re}), Prandtl number (N_{Pr}), the Nusselt number (N_{Nu}), and the h value for the fluid around the sample were expressed by following equations, respectively:

$$N_{Re} = \frac{Lvp}{\mu} \tag{7}$$

$$N_{Pr} = \frac{C_p \mu}{k} \tag{8}$$

for the laminar region,

$$N_{\mathrm{Nu}} = 0.664 N_{Re,L}^{1/2} N_{Pr}^{1/3} \tag{9a}$$

for the turbulent region,

$$N_{\mathrm{Nu}} = 0.0296 N_{Re,L}^{4/5} N_{Pr}^{1/3} \tag{9b}$$

$$h = \frac{N_{Nu} k}{L} \tag{10}$$

where ρ is the density, μ is the viscosity, v is the velocity, L is the average length of the longest side of the sample, Cp is the specific heat, and k is the thermal conductivity. Physical properties of water at the T_f are ρ = 986.42 kg/m^3, μ = 6.63x10^{-4} Pa·s, C_p = 4178.65 J kg^{-1} °C^{-1}, and k = 0.65 W m^{-1} °C^{-1}.

2.6. Evaluation of the validity of the simulation results

The transient temperature profiles resulted from the numerical simulation during the thermal treatment could be evaluated by comparing the experimental data. But, applying statistical analysis is a useful way to evaluate the validity of the simulation results. Generally, the validity of modeling results is evaluated with the root mean square error (RMSE).

RMSE was given by the following equation:

$$\mathrm{RMSE} = \sqrt{\frac{1}{N} \cdot \sum_{i=1}^{N} (T - T_{simulation})^2} \tag{11}$$

The temperature measured at geometric center of surimi paste during thermal treatment and those from the simulation were used to calculate the RMSE.

2.7. Statistical analysis

The results were presented as the average and standard deviation (SD) of each experiment conducted at least in duplicate and evaluated using SPSS Statistics 22 (SPSS Inc., Chicago, IL, USA). Analysis of variance (ANOVA) with Duncan test was used to determine statistical significance ($p < 0.05$). Stepwise multiple regression tool in SPSS Statistics 22 was used for developing and analyzing the empirical models. At each step of stepwise multiple regression, a predictor were enter or removed based on partial F-tests. F-to-enter and F-to-remove were 0.05 and 0.10, respectively.

3. RESULTS AND DISCUSSIONS

3.1. Density

The density of AP surimi paste at various moisture (76 to 84 %) and salt (0 to 3 %) contents at different temperatures are listed in Table 1. The density of AP surimi paste significantly decreased ($p < 0.05$) with increasing moisture and temperature at the same level of salt. The heat induced gelation or setting led to an increase in volume of the sample. The density changes of surimi paste is mainly due to the spatial arrangement of the native protein chains during the heat treatment (Ziegler and Acton 1984). More disordered arrangement of myofibrillar molecules in surimi paste caused the volume changes and eventually the volume of surimi paste increased after the heat induced gelation. Since the density of water in the surimi paste is lower than that of other components, mainly protein, the density of surimi paste decreased as the moisture content increased (AbuDagga and Kolbe 1997). The density of Pacific whiting (PW) surimi with different moisture contents (74 to 84%) and temperature (30, 60, and 90 °C) were in line with the results observed in the present study (AbuDagga and Kolbe 1997).

At a low temperature, for example 20 or 30 °C, the density of paste increased for all moisture content as the salt content increased, except 3% of salt at 84% of moisture content (Table 1). The increase of density might be because the addition of salt solubilizes more proteins and it causes the interaction between dissolved protein molecules in the paste. However, as the moisture content increased, the increment of density became smaller. That might be because the relative amount of protein in the paste on which the salt influences is smaller as the moisture content increases. It is an interesting observation that at a high temperature, such as 90 °C, the density decreased for all moisture content as the salt concentration increased. The temperature dependence of the density at varied salt content is in agreement with the previous study in that the changes in density of surimi (threadfin bream) at a high salt content (3%) was larger at high temperature (90 °C) (Kok and Park 2006). A multiple linear regression model for the density of AP surimi paste as a function of temperature (T), moisture (M) content, and salt contents (S) was suitably fitted from the experimental data ($R^2 = 0.92$) as follows:

$$\rho = 1450.20 - 0.47\ \mathrm{T} - 4.23\ \mathrm{M} + 5.40\ \mathrm{S} - 0.90\mathrm{TS} \quad (12)$$

Table 1: Density (ρ) of Alaska pollock surimi paste (kg/m^3).

T (°C)	76 M* (%)			80 M (%)			84 M (%)		
	0 S** (%)	1.5 S (%)	3 S (%)	0 S (%)	1.5 S (%)	3 S (%)	0 S (%)	1.5 S (%)	3 S (%)
20	1118.74±1.0$^{a***, C****, a*****}$	1125.95±1.3$^{a, B, a}$	1131.01±0.9$^{a, A, a}$	1101.12±0.8$^{a, C, b}$	1111.13±1.0$^{a, B, b}$	1116.06±1.1$^{a, A, b}$	1091.86±1.0$^{a, B, c}$	1099.58±0.9$^{a, A, c}$	1099.21±1.0$^{a, A, c}$
30	1114.96±0.7$^{b, B, a}$	1121.47±1.9$^{b, A, a}$	1120.86±0.5$^{b, A, a}$	1093.22±0.6$^{b, B, b}$	1106.13±0.8$^{b, A, b}$	1107.35±0.7$^{b, A, b}$	1088.04±0.8$^{b, B, c}$	1091.91±0.8$^{b, A, c}$	1086.00±0.4$^{b, C, c}$
60	1089.13±0.5$^{d, C, a}$	1097.9±0.3$^{d, d, A, a}$	1094.07±0.4$^{c, B, a}$	1070.09±0.2$^{c, B, b}$	1079.26±0.1$^{c, A, b}$	1079.15±0.4$^{c, A, b}$	1064.34±0.9$^{c, B, c}$	1065.65±0.1$^{c, A, c}$	1055.98±0.8$^{c, C, c}$
90	1092.36±0.9$^{c, B, a}$	1099.81±0.7$^{c, A, a}$	1090.24±0.7$^{d, C, a}$	1068.27±0.7$^{d, B, b}$	1072.50±0.9$^{d, A, b}$	1061.52±1.1$^{d, C, b}$	1056.99±0.8$^{d, A, c}$	1049.13±0.4$^{d, B, c}$	1010.03±0.2$^{d, C, c}$

*M: moisture content

**S: salt content, ±Standard deviations (%)

*** Different superscript small letters denote significant differences ($p < 0.05$) in each row at the same moisture content.

3.2. Specific heat

Table 2: Specific heat (C_p) of Alaska pollock surimi paste (J·kg^{-1}·°C^{-1}).

T (°C)	76 M* (%)			80 M (%)			84 M (%)		
	0 S** (%)	1.5 S (%)	3 S (%)	0 S (%)	1.5 S (%)	3 S (%)	0 S (%)	1.5 S (%)	3 S (%)
25	3500.63±2.2$^{h***, A****, c*****}$	3495.31±3.6$^{h, A, c}$	3483.17±3.9$^{h, B, b}$	3540.78±1.6$^{h, A, b}$	3532.97±2.5$^{g, B, b}$	3478.24±1.8$^{g, C, b}$	3603.73±1.7$^{h, A, a}$	3549.68±1.4$^{h, C, a}$	3556.16±2.2$^{h, B, a}$
30	3608.38±2.7$^{g, A, b}$	3524.52±3.5$^{g, C, c}$	3594.92±2.7$^{f, B, a}$	3587.58±2.4$^{g, A, c}$	3532.27±2.3$^{g, B, b}$	3517.00±2.3$^{f, C, c}$	3677.16±3.4$^{g, A, a}$	3656.62±2.4$^{g, B, a}$	3584.94±2.0$^{g, C, b}$
40	3703.23±2.6$^{f, A, c}$	3604.78±2.5$^{f, B, c}$	3572.19±1.6$^{g, C, c}$	3722.81±1.8$^{e, A, b}$	3618.56±1.6$^{f, C, b}$	3670.74±1.6$^{d, B, b}$	3740.35±2.9$^{f, A, a}$	3690.94±1.9$^{f, B, a}$	3691.75±1.7$^{f, B, a}$
50	3743.54±2.5$^{d, A, b}$	3643.27±1.0$^{e, B, c}$	3631.28±2.4$^{e, C, c}$	3718.52±0.8$^{f, A, c}$	3654.67±2.1$^{e, C, b}$	3661.34±2.1$^{e, B, b}$	3799.51±2.0$^{e, A, a}$	3741.82±1.9$^{e, B, a}$	3709.17±1.8$^{e, C, a}$
60	3737.52±2.0$^{e, A, c}$	3710.98±1.1$^{d, B, c}$	3672.80±2.0$^{d, C, c}$	3813.51±0.4$^{d, A, b}$	3756.22±1.8$^{d, C, b}$	3765.44±2.2$^{c, B, b}$	3899.92±1.1$^{d, A, a}$	3871.97±3.1$^{d , B, a}$	3865.60±2.2$^{d, C, a}$
70	3831.50±1.6$^{c, B, c}$	3850.56±1.7$^{c, A, c}$	3829.54±2.6$^{c, B, b}$	3930.79±1.7$^{c, A, b}$	3925.97±1.5$^{c, B, a}$	3763.42±2.4$^{c, C, c}$	3965.09±1.6$^{c, A, a}$	3918.37±1.1$^{c, B, b}$	3963.84±3.0$^{c, A, a}$
80	3906.92±1.0$^{b, B, c}$	3898.33±2.1$^{b, C, c}$	4028.03±2.1$^{b, A, b}$	4135.02±2.3$^{b, A, a}$	3953.50±2.3$^{b, C, b}$	4021.38±1.0$^{b, B, c}$	4114.61±2.7$^{b, A, b}$	4008.26±3.5$^{b, B, a}$	4106.07±3.1$^{b, B, a}$
90	4022.12±2.3$^{a, B, c}$	3976.58±3.1$^{c, C, c}$	4072.55±3.9$^{a, A, c}$	4154.02±2.8$^{a, A, b}$	4032.64±3.6$^{a, B, b}$	4152.46±2.5$^{a, A, b}$	4184.68±2.9$^{a, B, a}$	4184.55±0.7$^{a, B, a}$	4232.51±2.2$^{a, A, a}$

*M: moisture content

**S: salt content, ±Standard deviations (%)

*** Different superscript small letters denote significant differences ($p < 0.05$) in each row at the same moisture content.

**** Different superscript capital letters denote significant differences ($p < 0.05$) in each column at the same moisture content.

***** Different superscript small letters denote significant differences ($p < 0.05$) at different moisture content.

The specific heat of AP surimi paste with different moisture and salt contents was measured at different temperature (Table 2). Generally, the specific heat of a solid is highly dependent on temperature (Engel and Reid 2006). The specific heat with 76, 80, and 84% moisture contents with 1.5% salt content increased from 3495.31 to 3976.58, 3532.97 to 4032.64, and 3549.68 to 4184.55 J·kg^{-1}·C^{-1}, respectively, during heating (25 to 90 °C).

Increasing the moisture content significantly increased the specific heat of AP surimi ($p < 0.05$). Due to the high specific heat of water, the higher specific heat was observed at the higher moisture contents in food (Sopade and LeGrys 1991, Noel and Ring 1992, Taiwo et al. 1996). As salt content increased, the specific heat slightly decreased at lower temperatures (25-60 °C) (Table 2). According to Solomon et al. (2002), the hydrogen bonds that form between water molecules can store heat as potential energy of vibration in water. However, when salt is added to water, the sodium chloride ions interact with the water molecules, which results in the reduction of specific heat. But, the interaction might be decreased in the range of gelation temperature as the heat-induced gelation occur. Thus, the effect of salt on the specific heat of AP surimi paste can be explained by interacting the sodium chloride ions with the water and protein molecules. Interestingly, the specific heat of AP and PW surimi pastes showed the same order of magnitude, although they are originated from different species. The specific heat of PW surimi paste at 80% moisture content was varied from 3542 to 4033 J·kg^{-1}·C^{-1} over the temperature range of 25–90 °C (AbuDagga and Kolbe 1997).

A linear model for the specific heat of AP surimi paste as a function of temperature (T) and moisture (M) content, and salt contents (S) was fitted based on the experimental data:

$$C_p = 2208.48 + 8.71\ \mathrm{T} + 13.93\ \mathrm{M} - 14.13\ \mathrm{S} \quad (13)$$

Although the linear regression did not accommodate the denaturation peaks where the denaturation and gelation occur (Lee and Yoon 2016), it has a good overall fit with an R^2 of 0.97, and could be considered a workable model to support the heat transfer governing equation.

3.3. Thermal conductivity

Table 3: Thermal conductivity (*k*) of Alaska pollock surimi paste (W·m^{-1}·°C^{-1}).

T (°C)	76 M* (%)			80 M (%)			84 M (%)		
	0 S** (%)	1.5 S (%)	3 S (%)	0 S (%)	1.5 S (%)	3 S (%)	0 S (%)	1.5 S (%)	3 S (%)
25	0.544±0.003$^{g***, B****, c*****}$	0.549±0.00.3$^{g, A, b}$	0.549±0.004$^{g, A, b}$	0.565±0.003$^{g, A, a}$	0.544±0.002$^{h, B, b}$	0.545±0.003$^{f, C, b}$	0.556±0.003$^{g, A, b}$	0.561±0.003$^{h, A, a}$	0.557±0.003$^{h, A, a}$
30	0.544±0.003$^{g, B, c}$	0.558±0.004$^{f, A, b}$	0.559±0.003$^{f, A, b}$	0.561±0.003$^{g, B, b}$	0.569±0.002$^{g, A, a}$	0.548±0.004$^{f, C, c}$	0.578±0.003$^{f, A, a}$	0.568±0.003$^{g, B, a}$	0.573±0.003$^{g, AB, a}$
40	0.576±0.003$^{f, A, b}$	0.546±0.003$^{g, B, b}$	0.570±0.005$^{e, A, b}$	0.581±0.004$^{f, B, b}$	0.588±0.002$^{f, A, a}$	0.584±0.004$^{e, AB, a}$	0.594±0.003$^{e, A, a}$	0.588±0.003$^{f, A, a}$	0.590±0.002$^{f, A, a}$
50	0.584±0.003$^{e, A, c}$	0.566±0.003$^{e, C, b}$	0.572±0.002$^{e, B, c}$	0.606±0.003$^{e, A, a}$	0.595±0.003$^{e, B, a}$	0.585±0.004$^{e, C, b}$	0.594±0.003$^{e, B, b}$	0.593±0.001$^{e, B, a}$	0.609±0.004$^{e, A, a}$
60	0.594±0.003$^{d, A, c}$	0.589±0.004$^{d, A, c}$	0.594±0.003$^{d, A, c}$	0.615±0.002$^{d, AB, b}$	0.619±0.003$^{d, A, b}$	0.611±0.00.3$^{d, B, b}$	0.649±0.004$^{d, A, a}$	0.647±0.003$^{d, A, a}$	0.643±0.003$^{d, A, a}$
70	0.630±0.004$^{c, B, c}$	0.646±0.004$^{c, A, b}$	0.646±0.002$^{c, A, b}$	0.645±0.004$^{c, A, b}$	0.628±0.003$^{c, B, c}$	0.641±0.003$^{c, A, b}$	0.682±0.002$^{c, A, a}$	0.671±0.003$^{c, B, a}$	0.667±0.004$^{c, B, a}$
80	0.703±0.005$^{b, A, c}$	0.683±0.004$^{b, B, c}$	0.671±0.004$^{b, C, c}$	0.712±0.002$^{b, B, b}$	0.699±0.002$^{b, C, b}$	0.718±0.004$^{b, A, b}$	0.761±0.004$^{b, A, a}$	0.750±0.004$^{b, B, a}$	0.745±0.004$^{b, B, a}$
90	0.743±0.004$^{a, A, c}$	0.746±0.005$^{a, A, c}$	0.750±0.004$^{a, A, c}$	0.772±0.005$^{a, A, b}$	0.767±0.005$^{a, A, b}$	0.775±0.004$^{a, A, b}$	0.808±0.002$^{a, A, a}$	0.791±0.003$^{a, B, a}$	0.805±0.005$^{a, A, a}$

*M: moisture content

**S: salt content, ±Standard deviations (%)

*** Different superscript small letters denote significant differences ($p < 0.05$) in each row at the same moisture content.

**** Different superscript capital letters denote significant differences ($p < 0.05$) in each column at the same moisture content.

***** Different superscript small letters denote significant differences ($p < 0.05$) at different moisture content.

The thermal conductivity of AP surimi paste with different salt and moisture contents was measured at different temperature (Table 3). Thermal conductivity was significantly dependent on the temperature as well as compositions in food. Especially for surimi paste, the moisture content in the paste is a major variable for the changes of thermal conductivity during heating. Compared to the moisture content in the surimi paste, the salt content showed no significant influence on the thermal conductivity. This result is in agreement with other studies on blending of salt with meat (Zhang et al. 2007, Marcotte et al. 2008) and the surimi paste prepared with pacific whiting (AbuDagga and Kolbe 1997). Zhang et al. (2007) also reported that the level of added salt had no effect ($p < 0.05$) on the measured the thermal conductivity of the meat blends. Similarly, the thermal conductivity of PW (80% w.b.) ranged from 0.536 to 0.683 $W \cdot m^{-1} \cdot °C^{-1}$ over the temperature range of 25 to 80 °C (AbuDagga and Kolbe 1997). The temperature dependence of thermal conductivity of surimi paste is in line with previous studies on the thermal conductivity behavior of other muscle foods (Marcotte et al. 2008).

To develop an empirical model for thermal conductivity of AP surimi, a stepwise multiple regression was conducted. This process is continued only if additional variables show a statistical significance to the regression equation. The empirical model can be written as:

$$k = 0.34 + 4.57 \times 10^{-5}\, T^2 + 3.67 \times 10^{-5}\, M^2 - 2.46 \times 10^{-5} TM \qquad (14)$$

As shown in eqn. 15, salt content was removed from the empirical model by the stepwise regression. The model with second degree terms of both temperature and moisture content satisfactorily predicted thermal conductivity of AP with an R^2 of 0.98. Our study concluded that the changes in thermal conductivity was highly dependent on the moisture content than salt content within our experimental range (Table 3).

The contour plots of thermal diffusivity of surimi paste during heating from 30 °C to 90 °C showed a strong moisture content dependence compared to salt content (Fig. 2.). As expected, the thermal diffusivity of AP surimi paste significantly increased with increasing temperature and moisture content while the salt content did not affect significantly the thermal diffusivity values. Thus, more comprehensive understanding of heat transfer of surimi paste during thermal processing could be obtained by analyzing the thermal diffusivity. The temperature and moisture dependency of thermal diffusivity of AP surimi paste is in agreement with previous studies on the thermal diffusivity behavior of other foods (Tansakul and Chaisawang 2006, Yang et al. 2002).

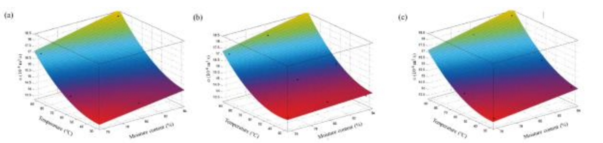

Figure 2: Surface plots of the thermal diffusivity (α) of AP surimi paste at (a) 0, (b) 1.5 and (c) 3% salt content.

3.4. Comparison of simulated and experimental temperature profiles of AP surimi pastes

The effect of the mesh size in the simulation geometry on the simulation of transient temperature profile of AP surimi paste during thermal processing was examined by comparing RMSE estimated at 80% moisture content and 1.5% salt content (Fig. 3).

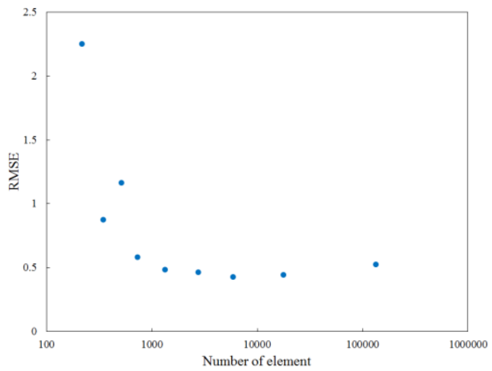

Figure 3: The RMSE result of AP surimi at 80% moisture content and 1.5% salt content at different number of element.

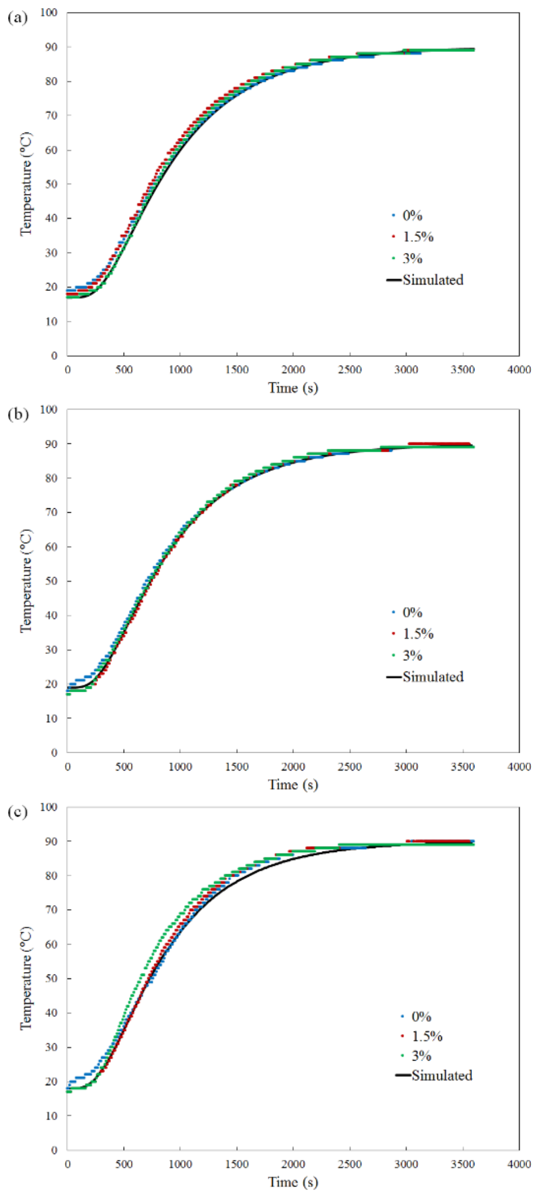

Figure 4: Temperature profiles of surimi pastes between measurement and CFD predictions (1.5% salt) for constant temperature (90 °C) water bath heating at (a) 76, (b) 80 and (c) 84% moisture content.

As the mesh size decreased from 10 mm to 1 mm, the number of element increased from 125 to 125000. At the lowest number of element, RMSE value was 2.26 and RMSE values were decreased as number of element increased. But, there was no significant differences in the range from 5 mm to 1 mm mesh size. As excess high mesh quality is inefficient for calculation time and the 3 mm mesh size (4913 elements) showed the lowest RMSE value in the range examined, the 3mm mesh size were used for the further analysis.

The transient temperature profiles at the center of the geometry from experiment and simulation were shown in Fig. 4. Since the salt content did not influence the thermal properties significantly, only 1.5 % of salt content was used for the validation. The transient temperature profiles at the center of the geometry from experiment and simulation were shown in Fig. 4. Since the salt content did not influence the thermal properties significantly, only 1.5 % of salt content was used for the validation. During convection heating using a water bath, the surimi sample with 76 % moisture with 1.5 % salt reached at the temperature of heating medium at 2990s, while the surimi samples with 80 and 84 % moisture took 2850 and 2420s, respectively. The sample with higher moisture content had a higher heating rate because it has a higher thermal conductivity (AbuDagga and Kolbe 1997). Because the specific heat also increases with moisture content, the high moisture content cannot increase the heating rate as much as the heat conductivity increased (AbuDagga and Kolbe 2000). Similarly, at 0 and 3% of salt contents, the surimi samples with 76, 80, and 84 of moisture contents reached at the heating medium temperature at 3140, 2880, and 2650s and 2980, 2780, and 2410s respectively.

To validate the use of the empirical models of temperature dependence of thermal properties for simulation model, the simulation models with constant values of properties measured at 30 °C (model A) and the simulation models with properties considering the sol-gel phase transition region (model B) were also evaluated. The RMSE values of each simulation calculated using eq. (11) is summarized in Table 4 and also the temperature distributions obtained from the model A, B and C at 84% moisture content and 1.5% salt contents were represented in Fig. 5. Since the thermal properties measured at 30 °C were the lowest value during heating, the temperatures in the transient temperature profile were lower than the actual values. Additionally, the RMSE of model A showed the highest RMSE among the three models. The RMSE values from the model A ranged from 1.87 to 2.32 °C. For the model B, the mean temperature for three temperature regions (15-40 °C, 40-50 °C and 50-90 °C) were 26.79 °C (0-580s), 45.22 °C (580-770s) and 82.06 °C (770-3600s), respectively. With consideration for the sol-gel phase transition, the RMSE of model B (1.01 to 1.58 °C) showed lower than that of Model A (1.87 to 2.32 °C)).

Table 4: Root mean square error (RMSE) of simulation and averaged experiment temperature profiles after convection heating.

	76 M*			80 M			84 M		
	Model A***	Model B****	Model C*****	Model A	Model B	Model C	Model A	Model B	Model C
0 S**	2.04	1.11	0.67	2.21	1.24	0.59	2.01	1.58	0.87
1.5 S	2.21	1.28	0.83	1.87	1.01	0.43	2.21	1.16	0.69
3 S	2.32	1.48	1.22	2.14	1.32	0.98	2.74	1.05	1.11

*M: moisture content (%).
**S: salt content (%).
***Model A: Simulation model with constant value of thermal properties at 30 °C.
****Model B: Simulation model with consideration the phase transition.
*****Model C: Simulation model with temperature-dependent functions of thermal properties.

The transient temperature profile obtained from the model B showed higher than those of actual values. It might be due to the average thermal properties were mainly estimated from the high temperature region that is the temperature above the sol-gel transition temperature. The mean thermal properties estimated in the high temperature region dominated the heat transfer simulation and such high value of thermal properties in the simulation resulted in the high temperature profile. The RMSE of the model C (0.43 to 1.22 °C) showed the lowest values. This demonstrated that the temperature dependent thermal property functions needs to be coupled with the heat transfer model to predict an accurate transient temperature profile of surimi paste during heating. The slowest heating zone evaluated different simulation models (A, B, and C) were shown in Fig. 5. The simulation results clearly demonstrated that the model A and B will cause a lack of heating and an overheating, respectively. The slowest heating zone of product have to be provide adequate heat treatment to ensure that the detrimental effect of microorganisms inactivated while preventing the degradation of food quality and its nutritive properties from excessive heating. Therefore, simulation model should be developed as accurate as possible. The thermal properties of AP surimi and the simulation method applied in this study may be useful in design of processing equipment, in process calculations of heating and cooling rates or times, and in calculating the process energy requirements, and also in the development of new processing techniques for surimi seafood products (Belibagli et al. 2003).

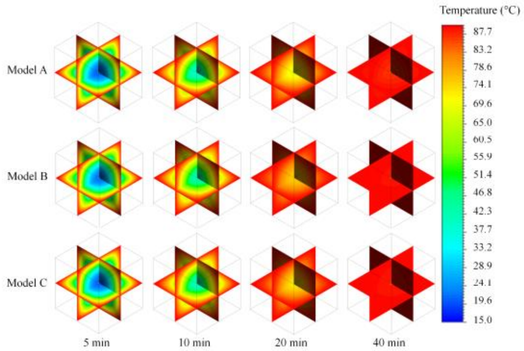

Figure 5: Estimation of the temperature distribution of the AP surimi at 84% moisture content and 1.5 % salt content during convective heating at 90 °C.

4. CONCLUSIONS

Density, specific heat, and thermal conductivity of AP surimi paste at varied moisture and salt contents have been measured and modelled in the temperature range 20-90°C. The density of AP surimi paste significantly decreased (p < 0.05) with increasing moisture content and temperature, and the density was slightly dependent on salt content. Specific heat and thermal conductivity increased with an increase in moisture content and temperature. Contrary to the expectations, the proportion of salt did not have any significant effect on the thermal conductivity. Thermal conductivity was most suitably fitted with a quadratic equation with an R^2 value of 0.98. The empirical models adequately predicted the thermal properties of AP surimi up on the moisture and salt content and the temperature. It was an interesting observation that the thermal properties of AP surimi were close to those of Pacific whiting surimi within our experimental range. It implies that the mixing two different species might be possible in the commercial processing with minimum effort of adjusting the existing process conditions. These models made of empirical measurements were validated by applying the thermal property models for the simulation. The RMSE values for the simulation model with empirical model ranged from 0.43 °C to 1.22 °C in AP surimi pastes while the RMSE values for the simulation model with constant value of each property at 30 °C (model A) and the simulation model with consideration for the sol-gel phase transition (model B) ranged from 1.87 °C to 2.32 °C and 1.01 to 1.58 °C, respectively. Simulated temperature profile of model C was found to be in good agreement with experimental temperature profile. Therefore, the simulation models with the empirical models of thermal properties can be used to identify cold point locations and can be used by food product developers for optimizing food composition and process design.

ACKNOWLEDGMENTS

This study has been worked with the support of a research grant of Kangwon National University in 2016.

REFERENCES

AbuDagga Y., Kolbe E., 1997. Thermophysical properties of surimi paste at cooking temperature. Journal of Food Engineering, 32(3), 325-337.

Abudagga Y., Kolbe E., 2000. Analysis of heat transfer in surimi paste heated by conventional and ohmic means. Journal of Aquatic Food Product Technology, 9(2), 43-54.

Anadharamakrishnan C., 2003. Computational Fluid Dynamics (CFD): Applications for the food industry. Indian Food Industry, 22(6), 62-68.

Augusto P.E., Soares B., Chiu M.C., Goncalves L.A., 2012. Modelling the effect of temperature on the lipid solid fat content (SFC). Food Research International, 45(1), 132-135.

Belibagli K.B., Speers R.A., Paulson A.T., 2003. Thermophysical properties of silver hake and mackerel surimi at cooking temperatures. Journal of Food Engineering, 60(4), 439-448.

Fontana A.J., Varith J., Ikediala J., Reyes J., Wacker B., 1999. Thermal properties of selected food using a dual needle heat-pulse sensor. In: ASAE Meeting Presentation.

Fukushima H., Okazaki E., Fukuda Y., Watabe S., 2007. Rheological properties of selected fish paste at selected temperature pertaining to shaping of surimi-based products. Journal of Food Engineering, 81(2), 492-499.

Geankoplis C.J., 2003. Transport processes and separation process principles: (includes unit operations) (4th ed.). Upper Saddle River, NJ, USA: Prentice Hall Press, 1056.

Guenneugues P., Morrissey M.T., 2005. Surimi resources. In: Park J.W., ed. Surimi and surimi seafood (2nd ed.). Boca Raton, FL, USA: CRC Press, 3-32.

Hong Y.K., Uhm J.T., Yoon W.B., 2014. Using Numerical Analysis to Develop and Evaluate the Method of High Temperature Sous-Vide to Soften Carrot Texture in Different-Sized Packages. Journal of Food Science, 79(4), 546-561.

Karunakar B., Mishra S.K., Bandyopadhyay S., 1998. Specific heat and thermal conductivity of shrimp meat. Journal of Food Engineering, 37(3), 345-351.

Kok T.N., Park J.W., 2006. Elucidating factors affecting floatation of fish ball. Journal of Food Science, 71(6), 297-302.

Lee M.G., Yoon W.B., 2016. Developing an effective method to determine the heat transfer model in fish myofibrillar protein paste with computer simulation considering the phase transition on various dimensions. International Journal of Food Engineering, 12(9), 889-900.

Mahapatra A.K., Mi S.L., Isang E.M., 2013. Effect of moisture content on thermal properties of cowpea

flours. Agricultural Engineering International: CIGR Journal, 15(2), 251-255.
Marcotte M., Taherian A.R., Karimi Y., 2008. Thermophysical properties of processed meat and poultry products. Journal of Food Engineering, 88(3), 315-322.
Mariani V.C., Lina A.G.B., Coelho L.S., 2008. Apparent thermal diffusivity estimation of the banana during drying using inverse method. Journal of Food Engineering, 85(4), 569-579.
Mohan V.P.C., Talukdar P., 2010. Three dimensional numerical modeling of simultaneous heat and moisture transfer in a moist object subjected to convective drying. International Journal of Heat and Mass Transfer, 53(21-22), 4638-4650.
Noel T.R., Ring S.G., 1992. A study of the heat capacity of starch/water mixtures. Carbohydrate Research, 227, 203-213.
Norton T., Sun D.W., 2006. Computational fluid dynamics (CFD)–an effective and efficient design and analysis tool for the food industry: a review. Trends in Food Science & Technology, 17(11), 600-620.
Park J.W., 2013. Surimi and surimi seafood (3rd ed.). Boca Raton, FL, USA: CRC Press.
Pitchai K., Chen J., Birla S., Gonzalez R., Jones D., Subbiah J., 2014. A microwave heat transfer model for a rotating multi-component meal in a domestic oven: development and validation. Journal of Food Engineering, 128, 60-71.
Scott G., Richardson P., 1997. The application of computational fluid dynamics in the food industry. Trends in Food Science & Technology, 8(4), 119-124.
Solomon E.P., Berg L.R., Martin D.W., 2002. Biology (6th ed.). Belmont, CA, USA: Thomson Brooks/Cole.
Sopade P.A., LeGrys G.A., 1991. Specific heat capacity of starch-sucrose systems. Food Control, 2(1), 50-52.
Tabilo-Munizaga G., Barbosa-Cánovas G.V., 2004. Color and textural parameters of pressured and heat-treated surimi gels as affected by potato starch and egg white. Food Research International, 37(8), 767-775.
Taiwo K.A., Akanbi C.T., Ajibola O.O., 1996. Thermal properties of ground and hydrated cowpea. Journal of Food Engineering, 29(3), 249-256.
Tansakul A., Chaisawing P., 2006. Thermophysical properties of coconut milk. Journal of Food Engineering, 73(3), 276-280.
Unklesbay N., Unklesbay K., Clarke A.D., 1999. Thermal properties of restructured beef snack sticks throughout smokehouse processing. LWT-Food Science and Technology, 32(8), 527-534.
Yang W., Sokhansani S., Tang J., Winter P., 2002. Determination of thermal conductivity, specific heat and thermal diffusivity of borage seeds. Biosystems Engineering, 82(2), 169-176.
Yongsawatdigul J., Park J.W., Kolbe E., 1995. Electrical conductivity of Pacific whiting surimi paste during ohmic heating. Journal of Food Science, 60(5), 922-925.
Zhang L., Lyng J.G., Brunton N.P., 2007. The effect of fat, water and salt on thermal and dielectric properties of meat batter and its temperature following microwave or radio frequency heating. Journal of Food Engineering, 80(1), 142-151.
Ziegler G.R., Acton J.C., 1984. Mechanisms of gel formation by proteins of muscle tissue. Food Technology, 38, 77-82.

AUTHORS BIOGRAPHY

Hyeon Woo Park is a second-year graduate student in Food Science and Biotechnology at Kangwon National University (KNU) in South Korea. He received his Bachelor's Degree in Food Science and Biotechnology from the Kangwon National University in 2015. His research interests include process optimization and new process design, surimi and surimi seafood processing and numerical and CFD simulation.

Dr. Park is a professor of Oregon State University since 1992. He was elected as IFT Fellow in 2007, which is the most prestigious recognition as a food scientist. He published 136 referred journal articles, 41 book chapters, and 3 patents. He offered over 100 invited speeches. Having devoted his entire professional career to fish protein (surimi) research and outstanding outreach in technology transfer, Dr. Jae Park has distinguished himself as an internationally renowned scientist in surimi research, education, and technology transfer. He received numerous awards to recognize his accomplishment regionally, nationally and internationally. He was recognized by IntraFish as 100 most powerful seafood executives in 2012. His most recent recognition was the 2016 IFT Bor S Luh International Award in Chicago in July, 2016.

Dr. Yoon is a professor at Kangwon National University (KNU) since 2008. He has a B.S. and M.S. in Food Science and Technology, and M.E. in Mechanical Engineering, and a Ph.D. major in Biological Systems Engineering and minor in Chemical Engineering. Before joining KNU, he worked in a processed food industry (associate director in Food R&D Center, CJ CheilJedang, Seoul, S. Korea) and a flavor company (Asia-Pacific regional marketing manager and Seafood specialist, Firmenich-Asia, Singapore). He has been working on food process engineering, food rheology and seafood processing for more than 13 years. His research interest includes gelation characterization of proteins and hydrocolloids, drying and powdering, high viscous fluid mechanics, heat and mass transfer during food processing, least cost formulation development, and computational fluid dynamics. He has so far published more than 80 articles in highly regarded journals in the field of food process engineering.